

Lecture notes on topological insulators

Ming-Che Chang

Department of Physics, National Taiwan Normal University, Taipei, Taiwan

(Dated: November 19, 2020)

Contents

I. Charge polarization, anomalous quantum Hall effect	1
A. Modern theory of charge polarization	1
1. Zak phase	2
2. Quantized charge pump	2
B. Rice-Mele model	3
C. Qi-Wu-Zhang model	4
D. Edge state in the Qi-Wu-Zhang model	5
References	7

I. CHARGE POLARIZATION, ANOMALOUS QUANTUM HALL EFFECT

In addition to the quantum Hall effect, Berry phase is essential to the calculation of charge polarization. It could also be a key ingredient in anomalous Hall effect. We illustrate these connections in this chapter.

A. Modern theory of charge polarization

The electric polarization \mathbf{P} of a *finite* crystal depends crucially on the charge accumulation near surfaces, and thus cannot be defined as a bulk property. On the other hand, for an *infinite* crystal, the calculation of \mathbf{P} , which is the expectation value of $q\mathbf{r}$, diverges.

For a crystal with periodic boundary condition (PBC), \mathbf{P} is generically not well defined. The reason is that, in a periodic solid, the electric polarization depends on one's choice of the unit cell (see Fig. 1). The theory of electric polarization in conventional textbooks applies only to solids consisting of well localized charges, such as ionic or molecular solids (**Clausius-Mossotti theory**). It fails, for example, in a covalent solid with bond charges such that no natural unit cell can be defined.

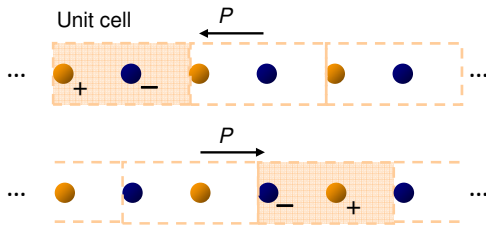


FIG. 1 For an infinite lattice, or a lattice with periodic boundary condition, the polarization is ill-defined. It depends on the choice of the unit cells.

A crucial observation made by R. Resta is that, even though the value of \mathbf{P} may be ambiguous, its *change* is well defined (Resta, 1992). It was soon pointed out by King-Smith and Vanderbilt that $\Delta\mathbf{P}$ has a deep connection with the Berry phase of the Bloch state (King-Smith and Vanderbilt, 1993).

To illustrate the modern theory of polarization, let's consider a one-dimensional (1D) lattice with periodic boundary condition. There are N lattice points located at $R_\ell = \ell a$ ($\ell \in Z$), and a is the lattice constant. The Fourier transformation of the Bloch state $\psi_{nk} = e^{ikx}u_{nk}$ is called the **Wannier state**,

$$|nR_\ell\rangle = \frac{1}{\sqrt{N}} \sum_{k=-\pi/a}^{\pi/a} e^{-ikR_\ell} |\psi_{nk}\rangle, \quad (1.1)$$

which is localized near a lattice point R_ℓ . The Bloch states form an orthonormal basis,

$$\langle \psi_{n'k'} | \psi_{nk} \rangle = \delta_{nn'} \delta_{kk'}. \quad (1.2)$$

Likewise, the Wannier states are also orthonormal to each other,

$$\langle n'R' | nR \rangle = \delta_{nn'} \delta_{RR'}. \quad (1.3)$$

Like Bloch states, the Wannier states $\{|n\mathbf{R}\rangle, \forall \mathbf{R}\}$ form a complete set of bases. A crucial difference is that the former is extended in space, while the latter is localized. With the Wannier states, one can avoid the problem of divergence when calculating the electric polarization.

In an insulator, electric polarization can be related to the *charge center* of the Wannier function,

$$P = q \sum_{\text{filled } n} \langle n0 | x | n0 \rangle, \quad q = -e \quad (1.4)$$

$$= \frac{q}{N} \sum_n \sum_{kk'} \langle u_{nk'} | e^{-ik'x} \frac{1}{i} \frac{\partial}{\partial k} (e^{ikx}) | u_{nk} \rangle \quad (1.5)$$

$$= \frac{q}{N} \sum_n \sum_{kk'} \langle u_{nk'} | e^{i(k-k')x} i \frac{\partial}{\partial k} | u_{nk} \rangle. \quad (1.6)$$

Decompose the x -integral as a sum of N unit-cell integrals, and write $x = ma + \tilde{x}$ ($\tilde{x} \in [0, a]$), it can be shown that (see Nomura, 2013, p.85)

$$\langle u_{nk'} | e^{i(k-k')x} i \frac{\partial}{\partial k} | u_{nk} \rangle = N \delta_{k,k'} \langle u_{nk} | i \frac{\partial}{\partial k} | u_{nk} \rangle_{\text{cell}} \quad (1.7)$$

$$= \delta_{k,k'} \langle u_{nk} | i \frac{\partial}{\partial k} | u_{nk} \rangle, \quad (1.8)$$

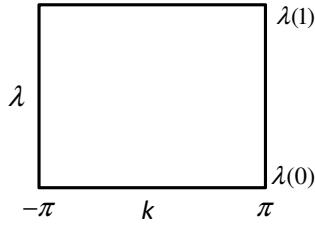


FIG. 2 The domain of Bloch momentum k and parameter λ is similar to a BZ of a two dimensional lattice.

where $\langle \dots \rangle_{cell}$ integrates over only one unit cell, and $N \langle \dots \rangle_{cell} = \langle \dots \rangle$ is used in the second equation. Therefore,

$$P = \frac{q}{N} \sum_n \sum_k \langle u_{nk} | i \frac{\partial}{\partial k} | u_{nk} \rangle \quad (1.9)$$

$$= qa \sum_n \int_{-\pi/a}^{\pi/a} \frac{dk}{2\pi} A_n(k). \quad (1.10)$$

Under a gauge transformation, $|u'_{nk}\rangle = e^{i\chi_{nk}} |u_{nk}\rangle$, where χ_{nk} is single-valued (mod 2π), the polarization contributed from band- n becomes,

$$P'_n = P_n - qa \frac{\chi_{n\pi/a} - \chi_{n-\pi/a}}{2\pi}. \quad (1.11)$$

Single-valuedness of χ_{nk} gives $\chi_{nk+2\pi/a} = \chi_{nk} + 2\pi ma$ ($m \in Z$), therefore,

$$P'_n = P_n - qma. \quad (1.12)$$

The polarization could change by qma under a gauge transformation. That is, only the fractional part of P_n (and P) is gauge invariant.

1. Zak phase

Note that the integral in Eq. (1.10) is nothing but the Berry phase around the BZ divided by 2π ,

$$P = qa \sum_n \frac{\gamma_n}{2\pi}. \quad (1.13)$$

The Berry phase of 1D Bloch state is first studied by Zak, 1989 and is called **Zak phase**. In addition to being gauge dependent, the value of Zak phase is also coordinate dependent (see Prob. 1), but the relative phases between energy bands are fixed.

For a 1D lattice with *space inversion* symmetry, if the origin is at a symmetric point, then the Zak phase can only be 0 or π , and P_n can only be 0 or $qa/2$. This can be understood as follows: It was shown earlier that if the lattice has space inversion symmetry, then (see Eq. (??))

$$A_n(-k) = -A_n(k). \quad (1.14)$$

Therefore, after the inversion,

$$P_n \rightarrow P'_n = qa \int_{-\pi/a}^{\pi/a} \frac{dk}{2\pi} A_n(-k) = -P_n. \quad (1.15)$$

Since P_n is allowed to have the freedom of changing by qma , the constraint given by the inversion symmetry is

$$P_n = -P_n \pmod{qa} \quad (1.16)$$

$$\rightarrow P_n = 0 \text{ or } q\frac{a}{2} \pmod{qa}. \quad (1.17)$$

Put it in another way, for a lattice with space-inversion symmetry, the charge center $\langle n0|x|n0 \rangle$ in a unit cell can only be at 0 or $a/2$. That is, on top of a lattice point or in the middle between two lattice points.

On the other hand, if there is no inversion symmetry, then γ_n (and P_n) can be any value. An experimental confirmation of the Zak phase with cold atoms can be found in Atala *et al.*, 2013.

2. Quantized charge pump

Even though P_n is gauge dependent, the change of polarization ΔP_n under an adiabatic and continuous deformation is gauge invariant and well-defined. From here on we consider only one filled band, and use λ to label the degree of ion displacement (with respect to ions of opposite charge). It varies from 0 to 1 as the ions shift adiabatically from an initial position to a final position.

The difference of polarizations between these two states is,

$$P(\lambda_2) - P(\lambda_1) = qa \int_{-\pi/a}^{\pi/a} \frac{dk}{2\pi} [A(k, \lambda_2) - A(k, \lambda_1)]. \quad (1.18)$$

The parameter λ defines a second dimension in addition to k . We can choose the parallel transport gauge (see Chap ??), such that along the λ -direction,

$$\langle u_{nk} | \frac{\partial}{\partial \lambda} | u_{nk} \rangle = 0, \quad (1.19)$$

then ΔP can be written as a (counter-clockwise) line integral around the rectangle in Fig. 2,

$$\Delta P = -\frac{qa}{2\pi} \oint d\mathbf{k} \cdot \mathbf{A}(\mathbf{k}), \quad \mathbf{k} \equiv (k, \lambda) \quad (1.20)$$

$$= -\frac{qa}{2\pi} \int d^2k F_z(\mathbf{k}), \quad (1.21)$$

where $F_z(\mathbf{k}) = \partial_k A_\lambda - \partial_\lambda A_k$, and $A_\lambda = i \langle u_{\mathbf{k}} | \partial_\lambda | u_{\mathbf{k}} \rangle$.

If $\lambda(1) = \lambda(0)$, then the rectangle is similar to a BZ, where opposite edges harbor the same states. Therefore, the integral of the Berry curvature is an integer ($\times 2\pi$), and

$$\Delta P = qaC_1. \quad (1.22)$$

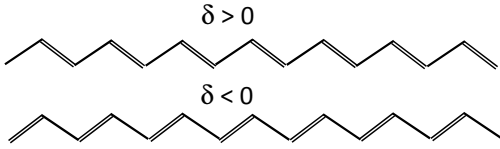


FIG. 3 Two different locations of double bonds in trans-polyacetylene.

That is, under a cyclic parametric variation, the charge transport is “quantized”. This fact can be utilized to build a **quantized charge pump** (Thouless *et al.*, 1982). However, be aware that even though the quantization is precise in the adiabatic limit, it is no longer so if the pumping is fast.

The analysis above is based on one-particle states in 1D. But the same scheme can be extended to real solids with electronic interactions in three dimensions. An essential alteration is to replace the one-particle states by the **Kohn-Sham orbitals** in the **density functional theory** (King-Smith and Vanderbilt, 1993).

B. Rice-Mele model

To illustrate the parametric charge pumping, we consider a dimerized 1D lattice (Rice and Mele, 1982),

$$H = \sum_{i=1}^{2N} (t_0 + (-1)^i \delta) (c_i^\dagger c_{i+1} + h.c.) - \sum_{i=1}^{2N} (-1)^i \Delta c_i^\dagger c_i, \quad (1.23)$$

where t_0 is the hopping amplitude between nearest neighbors, $\pm\delta$ modulate the hopping strength, $\pm\Delta$ are the on-site potentials for staggered sublattices, and $c_{2N+1} = c_1$ (PBC). The famous **Su-Shrieffer-Heeger model** (Su *et al.*, 1979) for polyacetylene is a special case of the Rice-Mele model with $\Delta = 0$ (see Fig. 3).

Since the lattice is dimerized, it is convenient to write $c_{i=2j-1}$ as c_j , $c_{i=2j}$ as d_j , and double the size of the unit cell. The Hamiltonian becomes,

$$H = \sum_{j=1}^N t_- (c_j^\dagger d_j + h.c.) + \sum_{j=1}^N \Delta c_j^\dagger c_j + \sum_{j=1}^N t_+ (c_{j+1}^\dagger d_j + h.c.) - \sum_{j=1}^N \Delta d_j^\dagger d_j, \quad (1.24)$$

where $t_{\pm} \equiv t_0 \pm \delta$. Expand c_j and d_j ,

$$c_j = \frac{1}{\sqrt{N}} \sum_k e^{ijak} c_k, \quad (1.25)$$

$$d_j = \frac{1}{\sqrt{N}} \sum_k e^{ijak} d_k, \quad (1.26)$$

where N is the total number of unit cells, and a is the

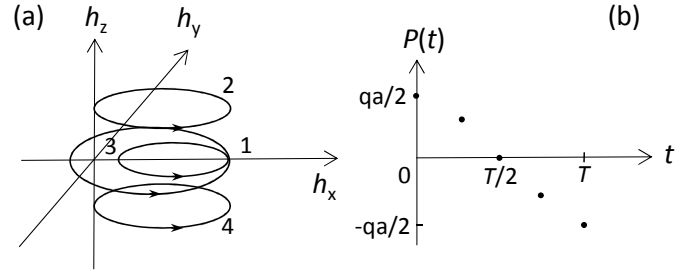


FIG. 4 (a) The trajectory of $\mathbf{h}(k)$ evolves in the order of 1, 2, 3, 4, when $t = 0, T/4, T/2, 3T/4$. (b) The evolution of electric polarization for the 4 steps in (a).

lattice constant, then

$$H = \sum_k (c_k^\dagger, d_k^\dagger) \begin{pmatrix} \Delta & t_- + t_+ e^{-iak} \\ t_- + t_+ e^{+iak} & -\Delta \end{pmatrix} \begin{pmatrix} c_k \\ d_k \end{pmatrix} = \sum_k (c_k^\dagger, d_k^\dagger) \mathbf{H}(k) \begin{pmatrix} c_k \\ d_k \end{pmatrix}. \quad (1.27)$$

One can write $\mathbf{H}(k) = \mathbf{h}(k) \cdot \boldsymbol{\sigma}$, in which

$$\mathbf{h}(k) = (t_- + t_+ \cos ka, t_+ \sin ka, \Delta). \quad (1.28)$$

The band energies are

$$\varepsilon_{\pm}(k) = \pm \left(\Delta^2 + 4t_0^2 \cos^2 \frac{ka}{2} + 4\delta^2 \sin^2 \frac{ka}{2} \right)^{1/2}. \quad (1.29)$$

The two energy bands touch at $(ka, \delta, \Delta) = (\pm\pi, 0, 0)$.

Note that the Hamiltonian \mathbf{H} has the same structure as the one for the spin-1/2 system in Eq. (??). $\mathbf{h}(k)$ plays the role of the magnetic field, and the two sublattices play the roles of the spin up/down degrees of freedom. Therefore, the Berry phase due to variation of parameters equals *half* of the solid angle extended by a closed path in the \mathbf{h} -space.

First, consider the SSH model with $\Delta = 0$: If $t_+ > t_-$ (i.e. $\delta > 0$), then when k runs across the first BZ, the trajectory of \mathbf{h} encircles the origin (path-1 in Fig. 4(a)). On the other hand, if $t_+ < t_-$ ($\delta < 0$), then \mathbf{h} follows path-3 that does not encircle the origin. Hence, the Berry phases for paths 1, 3 are $\pi, 0$ respectively. They indicate two different topological phases.

We now consider a cyclic variation,

$$(\delta(t), \Delta(t)) = \left(\delta_0 \cos 2\pi \frac{t}{T}, \Delta_0 \sin 2\pi \frac{t}{T} \right). \quad (1.30)$$

When t evolves through a period T , $\mathbf{h}(k)$ ($k \in [0, 2\pi/a]$) traverses paths 1, 2, 3, 4 and back to 1 in Fig. 4(a). After a full cycle, the polarization $P = qa\gamma/2\pi$ changes by $qa \pmod{qa}$, and a quantized charge q could be transported with a distance a (Fig. 4(b)). Experimental confirmations of the charge pumping related to the Rice-Mele model can be found in Lohse *et al.*, 2015, and Nakajima *et al.*, 2016.

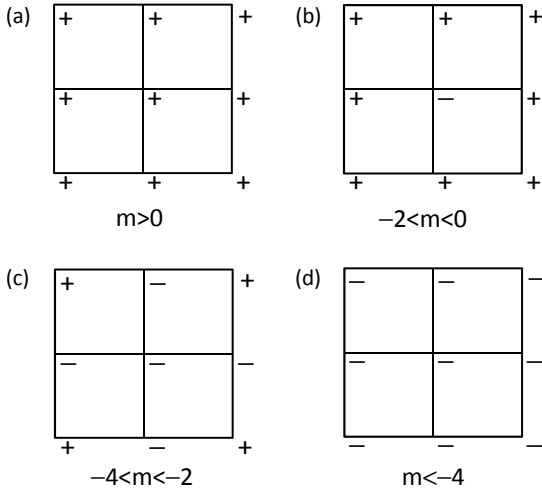


FIG. 5 Distribution of $\mathbf{h}(\mathbf{k})$ vectors in the BZ. Only the signs of $h_z(\mathbf{k})$ are shown.

C. Qi-Wu-Zhang model

In this section, we introduce a simple 2D model proposed by Qi, Wu and Zhang to illustrate the connection between Berry phase and quantized Hall conductivity (Qi *et al.*, 2006). The fermions are living on a 2D square lattice, and each lattice point is allowed to have two degrees of freedom (quasi-spin). The quasi-spin refers to the valence band with p -orbitals and the conduction band with s -orbitals. The QWZ Hamiltonian is given as,

$$\begin{aligned} \mathbf{H}(\mathbf{k}) &= \mathbf{H}_0 + \mathbf{H}_m + \mathbf{H}_{hy}, \\ \mathbf{H}_0 &= \varepsilon_0(\mathbf{k}) + \\ t &\begin{pmatrix} 2 - \cos k_x a - \cos k_y a & 0 \\ 0 & -(2 - \cos k_x a - \cos k_y a) \end{pmatrix}, \\ \mathbf{H}_m &= m \begin{pmatrix} 1 & 0 \\ 0 & -1 \end{pmatrix}, \\ \mathbf{H}_{hy} &= \lambda \begin{pmatrix} 0 & \sin k_x a - i \sin k_y a \\ \sin k_x a + i \sin k_y a & 0 \end{pmatrix}. \end{aligned} \quad (1.31)$$

\mathbf{H}_m is a mass term that opens an energy gap, and \mathbf{H}_{hy} is the hybridization between s - and p -orbitals.

In short,

$$\mathbf{H}(\mathbf{k}) = \varepsilon_0(\mathbf{k}) + \mathbf{h}(\mathbf{k}) \cdot \boldsymbol{\sigma}, \quad (1.32)$$

where

$$\mathbf{h}(\mathbf{k}) = \left(\lambda \sin k_x a, \lambda \sin k_y a, m + t \sum_{j=1}^2 (1 - \cos k_j a) \right). \quad (1.33)$$

The eigen-energies are,

$$\varepsilon_{\pm}(\mathbf{k}) = \varepsilon_0(\mathbf{k}) \pm |\mathbf{h}(\mathbf{k})|. \quad (1.34)$$

For simplification, we will set $t, a = 1$. It is not difficult

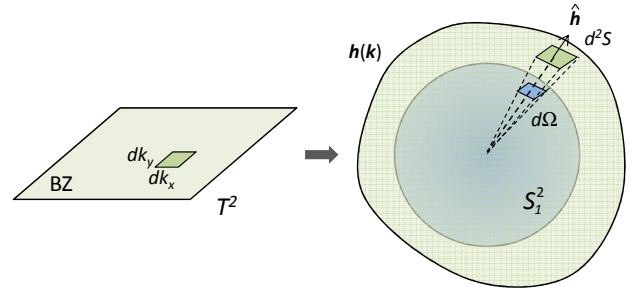


FIG. 6 Mapping a small area d^2k in the 2D BZ to a small area $d^2\mathbf{S}$ on the surface of $\mathbf{h}(\mathbf{k})$. Its solid angle $d\Omega$ is equal to the area of $\hat{\mathbf{h}} \cdot d^2\mathbf{S}$ projected on a unit sphere S^2_1 .

to see that,

$$\mathbf{k}_0 = 0 \rightarrow \varepsilon_{\pm}(\mathbf{k}_0) = \varepsilon_0 \pm m, \quad (1.35)$$

$$\mathbf{k}_0 = (\pi, 0), (0, \pi) \rightarrow \varepsilon_{\pm}(\mathbf{k}_0) = \varepsilon_0 \pm |m + 2|, \quad (1.36)$$

$$\mathbf{k}_0 = (\pi, \pi) \rightarrow \varepsilon_{\pm}(\mathbf{k}_0) = \varepsilon_0 \pm |m + 4|. \quad (1.37)$$

The energy gap closes at $m = 0, -2$, and -4 . We will see that the topology of the Bloch states changes at these critical points, when the energy gap closes.

The distribution of the $\mathbf{h}(\mathbf{k})$ vectors in the BZ changes when an energy gap closes, see Fig. 5. Depending on the value of m , there are four different regimes:

- 1) $m > 0$: $h_z(\mathbf{k}) > 0$ over the whole BZ.
- 2) $-2 < m < 0$: $h_z(\mathbf{k}) < 0$ near $\mathbf{k} = 0$.
- 3) $-4 < m < -2$: $h_z(\mathbf{k}) > 0$ near $\mathbf{k} = (\pi, \pi)$ (and its equivalent points).
- 4) $m < -4$: $h_z(\mathbf{k}) < 0$ over the whole BZ.

The \mathbf{h} in Eq. (1.32) is the “magnetic field” for the quasi-spin. In case (1), the magnetic field only sweeps over the northern hemisphere when \mathbf{k} scans over the BZ. According to the analysis in ??, we need only one gauge $\mathbf{A}^N(\mathbf{k})$ for the whole BZ. Therefore, the topology is expected to be trivial and the Hall conductivity $\sigma_H = 0$.

In cases (2) and (3), h_z changes sign, so that \mathbf{h} sweeps through the whole sphere, and two gauges, \mathbf{A}^N and \mathbf{A}^S are required to avoid the singularity. Therefore the topology is non-trivial and $\sigma_H \neq 0$.

Case (4) is similar to Case (1), but \mathbf{h} sweeps over the southern hemisphere only. The topology is again trivial and $\sigma_H = 0$.

The simple picture presented above can be verified by actual calculation of σ_H . First, we show that (Nomura, 2013)

$$F_z^{\pm}(\mathbf{k}) = \mp \frac{1}{2h^3} \mathbf{h} \cdot \frac{\partial \mathbf{h}}{\partial k_x} \times \frac{\partial \mathbf{h}}{\partial k_y}. \quad (1.38)$$

Pf: The Berry connections in \mathbf{k} -space are,

$$A_\ell^\pm(\mathbf{k}) = i\langle \mathbf{h}, \pm | \frac{\partial}{\partial k_\ell} | \mathbf{h}, \pm \rangle \quad (1.39)$$

$$= \frac{\partial h_\alpha}{\partial k_\ell} i\langle \mathbf{h}, \pm | \frac{\partial}{\partial h_\alpha} | \mathbf{h}, \pm \rangle \quad (1.40)$$

$$= \frac{\partial h_\alpha}{\partial k_\ell} a_\alpha^\pm(\mathbf{h}), \quad (1.41)$$

where \mathbf{a}^\pm are the Berry connections in \mathbf{h} -space. Therefore, the Berry curvatures in \mathbf{k} -space are,

$$F_z^\pm(\mathbf{k}) = \frac{\partial A_y^\pm}{\partial k_x} - \frac{\partial A_x^\pm}{\partial k_y} \quad (1.42)$$

$$= \frac{\partial}{\partial k_x} \left(\frac{\partial h_\beta}{\partial k_y} a_\beta^\pm \right) - \frac{\partial}{\partial k_y} \left(\frac{\partial h_\alpha}{\partial k_x} a_\alpha^\pm \right) \quad (1.43)$$

$$= \frac{\partial h_\alpha}{\partial k_x} \frac{\partial h_\beta}{\partial k_y} \left(\frac{\partial a_\beta^\pm}{\partial h_\alpha} - \frac{\partial a_\alpha^\pm}{\partial h_\beta} \right) \quad (1.44)$$

$$= \frac{\partial h_\alpha}{\partial k_x} \frac{\partial h_\beta}{\partial k_y} \varepsilon_{\alpha\beta\gamma} f_\gamma^\pm \quad (1.45)$$

$$= \mp \frac{1}{2h^3} \mathbf{h} \cdot \frac{\partial \mathbf{h}}{\partial k_x} \times \frac{\partial \mathbf{h}}{\partial k_y}, \quad (1.46)$$

in which $f_\gamma^\pm = \mp h_\gamma / 2h^3$ are the Berry curvatures in \mathbf{h} -space. End of proof.

Suppose the lower band is completely filled, and the upper band is empty, then

$$\sigma_H = \frac{e^2}{h} \frac{1}{2\pi} \int_{BZ} d^2k F_z^-(\mathbf{k}) \quad (1.47)$$

$$= \frac{e^2}{h} \frac{1}{4\pi} \int_{BZ} d^2k \frac{1}{h^3} \mathbf{h} \cdot \frac{\partial \mathbf{h}}{\partial k_x} \times \frac{\partial \mathbf{h}}{\partial k_y}. \quad (1.48)$$

In the integrand, $\hat{\mathbf{h}} \cdot \left(\frac{\partial \mathbf{h}}{\partial k_x} dk_x \right) \times \left(\frac{\partial \mathbf{h}}{\partial k_y} dk_y \right)$ is actually the area $\hat{\mathbf{h}} \cdot d^2\mathbf{S}$ on the \mathbf{h} -surface in Fig. 6. After being divided by h^2 , it becomes the solid angle $d\Omega$ extended by that area. Since the BZ is a closed surface (a 2D torus, or T^2), under a continuous mapping, it would map to a closed surface in \mathbf{h} -space (see Fig. 7). The integral in Eq. (1.48) gives the total solid angle extended by that \mathbf{h} -surface. For a closed surface, it must be an integer multiple of 4π , thus

$$\sigma_H = w \frac{e^2}{h}, w \in Z. \quad (1.49)$$

The integer w , which is equal to the first Chern number C_1 , is the number of times the \mathbf{h} -surface wraps over a unit sphere S_1^2 . It characterizes the topology of the mapping (and the Bloch states) and is called the **winding number** (or wrapping number). We emphasize that w is an integer only if the base space is a close surface (in this case, T^2), which requires the valence band to be completely filled (that is, an insulator).

The quantized Hall conductance in the QWZ model is a result of the ‘‘magnetization’’ m , not an external magnetic field (as in the case of the quantum Hall effect). It

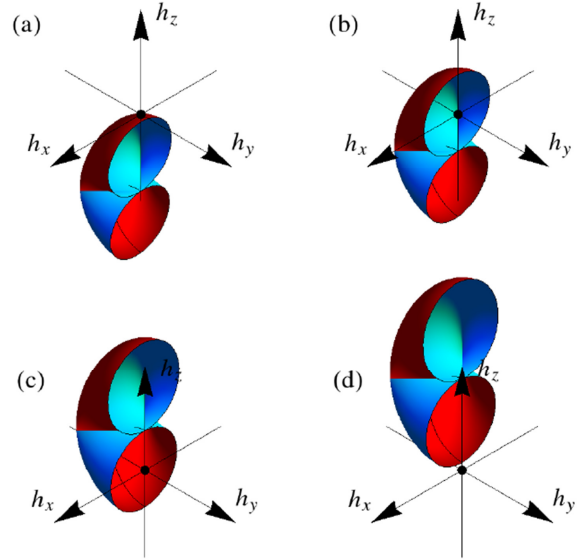


FIG. 7 The line segment $k_x \in [-\pi, \pi]$ in a BZ would map to a closed loop in \mathbf{h} -space. As one sweeps the line segment from $k_y = -\pi$ to $k_y = 0$, the loop in \mathbf{h} -space sweeps out a torus-like structure, as shown in the figures. Further advancement of k_y from 0 to π would map out another half of the torus (not shown for the sake of clarity). The winding number w depends on whether the origin is enclosed in the torus-like structure or not. In (a) and (d) (for $m < -4$ and $m > 0$), the origin is outside of the surface, so $w=0$. In (b) and (c) (for $m = -3$ and $m = -1$), the winding numbers are -1 and $+1$ respectively (not easily seen, though). [These figures are from [Asbóth et al., 2013](#)]

is called alternatively as the **quantum anomalous Hall effect** (QAHE). Their difference is that, in the QHE, the electron orbitals are quantized due to the external magnetic field; in the QAHE there is no orbital quantization, but only spin re-orientation due to m . A recent confirmation of the QAHE can be found in [Chang et al., 2013](#).

One could apply an external magnetic field to the QAH insulator (aka **Chern insulator**). Then there will be orbital quantization and Landau levels in energy spectrum. Interested readers can consult p. 103 of [Bernevig and Hughes, 2013](#) for more details.

D. Edge state in the Qi-Wu-Zhang model

Topological materials (insulators) have an important property: their surface states are stable against perturbations. They can be destroyed only if the energy gap of the bulk bands closes so that the topology of the electronic states is trivialized. In general, *the interface between two materials with different topologies would have robust interface states*. A heuristic explanation is as follows: to go from one material to another, the spatial-dependent energy gap (in the sense of the Thomas-Fermi approximation) needs to close near the interface, otherwise it

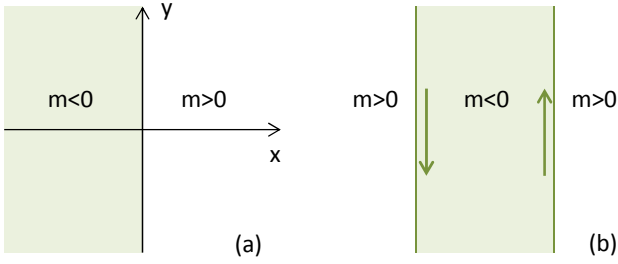


FIG. 8 (a) A topological phase occupies the left side of the space. (b) A finite sample with two boundaries. The edge states move in a definite direction along an edge.

is simply impossible for the topology to change. This gapless region is where the surface states reside.

Take the 2D QWZ model as an example. Divide the space to two parts where

$$m(x) \begin{cases} > 0 \text{ for } x > 0, \\ < 0 \text{ for } x < 0, \end{cases} \quad (1.50)$$

so that there is a 1D boundary along the y -axis (see Fig. 8(a)). For simplicity, consider only the small k limit,

$$\mathbf{H}(\mathbf{k}) = \varepsilon_0 + \begin{pmatrix} m & \lambda(k_x - ik_y) \\ \lambda(k_x + ik_y) & -m \end{pmatrix} + O(k^2). \quad (1.51)$$

The exact profile of $m(x)$ does not matter, as long as it is monotonic and smooth (compared to the electron wavelength λ). To solve for the surface states, one needs to re-quantize the Hamiltonian using the substitution $\mathbf{k} \rightarrow \frac{1}{i} \frac{\partial}{\partial \mathbf{r}}$, such that

$$\mathbf{H}(\mathbf{p}) = \varepsilon_0 + \begin{pmatrix} m(x) & \lambda \left(\frac{1}{i} \frac{\partial}{\partial x} - \frac{\partial}{\partial y} \right) \\ \lambda \left(\frac{1}{i} \frac{\partial}{\partial x} + \frac{\partial}{\partial y} \right) & -m(x) \end{pmatrix}. \quad (1.52)$$

The x -directions extend to infinity on both ends, and PBC is imposed along the y -direction.

We now solve the differential equation,

$$\mathbf{H}(\mathbf{p})\psi(x, y) = \varepsilon\psi(x, y). \quad (1.53)$$

Use the method of separation of variables and write

$$\psi(x, y) = \phi_1(x)\phi_2(y). \quad (1.54)$$

Since the y -direction is invariant under translation, a trivial solution is $\phi_2(y) = e^{ik_y y}$, a plane wave. Therefore, the equation for $\phi_1(x)$ is,

$$\begin{pmatrix} m(x) & \lambda \left(\frac{\partial}{\partial x} + k_y \right) \\ \lambda \left(\frac{\partial}{\partial x} - k_y \right) & -m(x) \end{pmatrix} \phi_1(x) = \varepsilon_e(k_y)\phi_1(x). \quad (1.55)$$

We can take a guess at a solution that is localized near the boundary,

$$\phi_1(x) = e^{-\frac{1}{\lambda} \int_0^x dx' m(x')} \begin{pmatrix} a \\ b \end{pmatrix}. \quad (1.56)$$

It can be verified as an eigenstate with eigenvalue $\varepsilon_e(k_y) = \lambda k_y$ if $(a, b) = (1, i)$. Furthermore, it decays to zero at $x \ll 0$ and $x \gg 0$, and has a peak at $x = 0$.

On the other hand, if

$$m(x) \begin{cases} > 0 \text{ for } x < 0, \\ < 0 \text{ for } x > 0, \end{cases} \quad (1.57)$$

then

$$\phi_1(x) = e^{\frac{1}{\lambda} \int_0^x dx' m(x')} \begin{pmatrix} 1 \\ -i \end{pmatrix}. \quad (1.58)$$

is a localized eigenstate with $\varepsilon_e(k_y) = -\lambda k_y$.

Therefore, in a sample with finite width (see Fig. 8(b)), the electrons on the right edge move with velocity $\frac{1}{\hbar} \frac{\partial \varepsilon_e}{\partial k_y} = \lambda/\hbar$; the ones on the left move with velocity $-\lambda/\hbar$. They are called **chiral edge states**. The two edges can be treated as independent only if the strip is wide enough (compared to the decay length of the edge state) so that the edge states on two sides do not couple with each other. In the small k_y limit, the energy dispersion $\varepsilon_e(k_y)$ of the edge states are linear in k_y . This is not so for larger k_y 's, where numerical calculation is required.

Exercise

1. The value of Zak phase depends on the choice of the origin. Under a shift of the origin,

$$\psi_k(x) \rightarrow \psi'_k(x) = \psi_k(x - d). \quad (1.59)$$

This leads to

$$u_k(x) \rightarrow u'_k(x) = u_k(x - d)e^{-ikd}. \quad (1.60)$$

Show that

$$\gamma \rightarrow \gamma' = \gamma + 2\pi \frac{d}{a}, \quad (1.61)$$

where a is the lattice constant.

2. The $\mathbf{h}(k)$ of SSH model traces out a loop in the \mathbf{h} -space when k runs through the first Brillouin zone.

(a) Show that the following expression gives the winding number of the loop around the origin,

$$w = \frac{1}{2\pi} \int_{BZ} dk \frac{1}{\hbar^2} \hat{\mathbf{z}} \cdot \mathbf{h} \times \frac{d\mathbf{h}}{dk}. \quad (1.62)$$

(b) The SSH Hamiltonian can be written as,

$$\mathbf{H}(k) = \begin{pmatrix} 0 & Q(k) \\ Q^*(k) & 0 \end{pmatrix}. \quad (1.63)$$

Find out $Q(k)$ and show that the following expression also gives the winding number of $\mathbf{h}(k)$ around the origin,

$$w = \frac{i}{2\pi} \int_{BZ} dk \frac{d}{dk} \ln Q(k). \quad (1.64)$$

3. Assume a SSH chain has two domains: $\delta(x) = -\delta_0 < 0$ for $x \ll 0$, $\delta(x) = \delta_0$ for $x \gg 0$, and $\delta(x)$ varies smoothly

and monotonically from $-\delta_0$ to δ_0 in between. We will find out a localized state that is trapped in this domain wall.

(a) The low-energy states are located near $ka = \pm\pi$. Write k as $\pi/a + q$, and expand $H(k)$ to linear order in q . This is the Hamiltonian in the continuum limit.

(b) Replace q with $(1/i)\partial/\partial x$ to requantize the H in (a), and find out the eigenstate $\psi_0(x)$ with zero energy.

Note: This problem is first studied in [Jackiw and Rebbi, 1976](#). A recent experimental study can be found in [Meier et al., 2016](#).

4. In Prob. 3 of Chap 2, we derived the effective Hamiltonian of an electron moving in a non-uniform magnetic field $\mathbf{B}(\mathbf{r}, t) = B_0 \hat{m}(\mathbf{r}, t)$,

$$\left[\frac{1}{2m} (\mathbf{p} - \hbar \mathbf{A}_n)^2 + \hbar V_n + \varepsilon_n \right] \psi_n = i\hbar \frac{\partial \psi_n}{\partial t}, \quad (1.65)$$

where V_n and \mathbf{A}_n can be found there.

(a) Show that an electron with spin up/down feels an effective electromagnetic field,

$$\tilde{E}_\alpha = \mp \frac{1}{2} \hat{m} \cdot \frac{\partial \hat{m}}{\partial r_\alpha} \times \frac{\partial \hat{m}}{\partial t}, \quad (1.66)$$

$$\tilde{B}_\gamma = \mp \frac{1}{4} \epsilon_{\alpha\beta\gamma} \hat{m} \cdot \frac{\partial \hat{m}}{\partial r_\alpha} \times \frac{\partial \hat{m}}{\partial r_\beta}. \quad (1.67)$$

As a result, an electron with velocity \mathbf{v} is subject to a force $\hbar(\tilde{\mathbf{E}} + \mathbf{v} \times \tilde{\mathbf{B}})$.

(b) A magnetic skyrmion is a topological spin texture in magnetic materials. Because of the exchange interaction, the spin texture has an effective magnetic field that can be identified with the $\mathbf{B}(\mathbf{r}, t)$ -field above. Show that a skyrmion moving rigidly (without change of shape) with velocity \mathbf{v}_s generates an effective electric field that is transverse to the direction of motion,

$$\tilde{\mathbf{E}} = -\mathbf{v}_s \times \tilde{\mathbf{B}}, \quad (1.68)$$

where $\tilde{\mathbf{B}}$ is the effective magnetic field of a static skyrmion.

References

- Asbóth, J. K., L. Oroszlány, and A. Pályi, 2013, Topological insulators, unpublished.
- Atala, M., M. Aidelsburger, J. T. Barreiro, D. Abanin, T. Kitagawa, E. Demler, and I. Bloch, 2013, *Nat. Phys.* **9**, 795.
- Bernevig, B. A., and T. L. Hughes, 2013, *Topological Insulators and Topological Superconductors* (Princeton University Press).
- Chang, C.-Z., J. Zhang, X. Feng, J. Shen, Z. Zhang, M. Guo, K. Li, Y. Ou, P. Wei, L.-L. Wang, Z.-Q. Ji, Y. Feng, et al., 2013, *Science* **340**(6129), 167.
- Jackiw, R., and C. Rebbi, 1976, *Phys. Rev. D* **13**, 3398.
- King-Smith, R. D., and D. Vanderbilt, 1993, *Phys. Rev. B* **47**, 1651.
- Lohse, M., C. Schweizer, O. Zilberberg, M. Aidelsburger, and I. Bloch, 2015, *Nat. Phys.* **12**, 350.
- Meier, E. J., F. A. An, and B. Gadway, 2016, *Nature Communications* **7**, 13986 EP, article.
- Nakajima, S., T. Tomita, S. Taie, T. Ichinose, H. Ozawa, L. Wang, M. Troyer, and Y. Takahashi, 2016, *Nat. Phys.* **12**, 296.
- Nomura, K., 2013, Fundamental theory of topological insulator, unpublished, written in Japanese.
- Qi, X.-L., Y.-S. Wu, and S.-C. Zhang, 2006, *Phys. Rev. B* **74**, 085308.
- Resta, R., 1992, *Ferroelectrics* **136**(1), 51.
- Rice, M. J., and E. J. Mele, 1982, *Phys. Rev. Lett.* **49**, 1455.
- Su, W. P., J. R. Schrieffer, and A. J. Heeger, 1979, *Phys. Rev. Lett.* **42**, 1698.
- Thouless, D., M. Kohmoto, M. Nightingale, and M. Den Nijs, 1982, *Phys. Rev. Lett.* **49**(6), 405.
- Zak, J., 1989, *Phys. Rev. Lett.* **62**, 2747.